TANG HUMANITAS MEDICINE

Original Article

Effect of KH-BaRoKer-SeongJangTang based on traditional medicine theory on longitudinal bone growth

Min-Ho Kim[1], Hyeonseok Jeong[2], Myungduek Park[2], Phil-Dong Moon[3,*]

1High-Enthalpy Plasma Research Center, Chonbuk National University, 664-14, 1Ga Deokjin-dong, Deokjin-gu, Jeonju 561-756, Republic of Korea; 2Kyungheebaroker Clinic of Korea Traditional Medicine, 1206 Ara tower, Seochodaero 77 gil 3, Seocho-gu, Seoul 137-856, Republic of Korea; 3Department of Pharmacology, College of Korean Medicine, Kyung Hee University, 1 Hoegi-dong, Dongdaemun-gu, Seoul 130-701, Republic of Korea

ABSTRACT

KH-BaRoKer-SeongJangTang (KBS) is a recently developed formulation by using traditional drugs considering traditional medical theory of Oriental books such as ShinNongBonChoGyeong and JuRye, which has been used to improve the growth of child in Korea. Although KBS is usually prescribed to many children who are in retard for their age, its pharmacological effects have not been fully understood in experimental models. The aim of this study was to evaluate the effects of KBS on bone growth. Growth plate thickness and bone parameters such as bone volume/tissue volume (BV/TV), trabecular thickness (Tb.Th), trabecular number (Tb.N), connection density (Conn.D), and total porosity were analyzed by means of microcomputed tomography. Serum insulin-like growth factor-I (IGF-I) levels were measured by enzyme-linked immunosorbent assay. Hepatic IGF-I mRNA expression was analyzed by real-time polymerase chain reaction. Phosphorylation of signal transducer and activator of transcription5 (STAT5) was investigated using Western blot analysis and immunohistochemistry. The thickness of growth plate was increased by KBS. BV/TV, Tb.Th, TbN, Conn.D, and total porosity were improved by KBS. Hepatic IGF-I mRNA and serum IGF-I levels were elevated by KBS. Phosphorylation of STAT5 was increased with administration of KBS. These results suggest that KBS would be helpful to children who are in retard for their age through the elevation of IGF-I.

Keywords growth plate, bone parameters, insulin-like growth factor-I, signal transducer and activator of transcription5

INTRODUCTION

In mammals, growth of long bones occurs at the growth plate, a cartilaginous structure present in tubular bones and vertebrae (Abad et al., 2002; Lui and Baron, 2011). The growth plate is a layer of cartilage present in growing long bones between the epiphysis and the metaphysis (Abad et al., 2002). The rate of longitudinal bone growth at the growth plate is controlled by a system of endocrine signals including growth hormone (GH), insulin-like growth factor-I (IGF-I), thyroid hormone, androgens and estrogens. If a child is undernourished, circulating IGF-I and thyroid hormone decline. In adolescents, undernutrition also causes decline in sex steroids. These endocrine changes suppress the bone growth (Lui and Baron, 2011). To reproduce the undernourishment, a low protein diet was used in mice. Protein-energy malnutrition (PEM) is a major form of malnutrition and is defined as an imbalance between food intake (protein and energy) and the amount that the body requires to ensure the most favorable growth and function (Fock et al., 2010).

GH is a major regulator of growth and development (de Vos et al., 1992). Actions of GH are initiated by binding to the GH receptor (GHR) on the cell surface (Brooks and Waters, 2010). Binding of GH to GHR activates receptor-associated intracellular tyrosine protein kinase Janus kinase 2 (JAK2), which phosphorylates signal transducer and activator of transcription 5 (STAT5). The phosphorylated STAT proteins translocate to the nucleus, where they bind to specific DNA sequences and regulate gene transcription (Le Roith et al., 2001). Among the signal cascades from the GHR, the JAK2-STAT5 pathway is regarded as a major pathway that mediates the action of GH on gene transcription in the liver (Davey et al., 1999; Rabkin et al., 2005). This pathway was shown to be responsible for the transcriptional action of GH on IGF-I (Woelfle et al., 2003). IGF-I is a mitogenic factor for various cells and plays an important role in cell growth and survival, and the majority of plasma IGF-I is biosynthesized in the liver (King et al., 2013; Weng et al., 2009; Youreva et al., 2013; Zhang et al., 2006).

KH-BaRoKer-SeongJangTang (KBS) is a recently developed formulation by using traditional drugs considering traditional medical theory of Oriental books such as ShinNongBonChoGyeong and JuRye, which has been used to improve the growth of child in Korea. Although KBS is usually prescribed to many children who are in retard for their age, its pharmacological effects have not been fully understood in experimental models. Thus, this study used a murine model to investigate how KBS and its constituents, arginine (Arg) and

*Correspondence: Phil-Dong Moon
E-mail: pdmoon@khu.ac.kr
Received April 18, 2014; **Accepted** May 22, 2014; **Published** May 31, 2014
doi: http://dx.doi.org/10.5667/tang.2014.0020

Table 1. Composition of Experimental Diets.[a]

Ingredients	Standard chow diet (g/kg diet)	PEM diet (g/kg diet)
Casein (> 85% protein)	200	40
Sucrose	100	100
Fiber	10	10
Corn oil	80	80
Mineral mixture[b]	40	40
Vitamin mixture[b]	10	10
L-Methionine	1.5	1.5
Choline Bitartrate	2.5	2.5
Cornstarch	556.5	716.5

Note: [a]Isocaloric diets providing 1716.3 kJ/100 g; [b]Mineral and vitamin mixtures were prepared according to the 1993 recommendations of the American Institute of Nutrition for adult mice (Reeves et al., 1993)

glutamine (Glu) affect the bone growth.

MATERIALS AND METHODS

Reagents

Arg, avidin-peroxidase, and bovine serum albumin were purchased from Sigma Chemical Co. (St. Louis, MO, USA). Anti-mouse IGF-I antibody, biotinylated anti- mouse IGF-I antibody, and recombinant mouse IGF-I were purchased from R&D Systems (Minneapolis, MN, USA). Phosphorylated (p)STAT5 antibody was purchased from Invitrogen Corp. (Camarillo, CA, USA). STAT5 antibody was purchased from Santa Cruz Biotechnology (Santa Cruz, CA, USA).

Animals and diets

Male ICR mice (4 weeks old) and diets were purchased from Dae-Han Experimental Animal Center (Eumsung, Republic of Korea), acclimated for 7 days, and then randomly assigned for 2 weeks to adequate protein (CON, 20% protein) or low protein diet (PEM, 4% protein) (Reeves et al., 1993). The protein source used was casein. Except for the protein content, the two diets were identical and isocaloric (Table 1). After 2 weeks, mice were divided into five groups, CON (adequate protein diet + distilled water (DW)-administered group); PEM (low protein diet + DW-administered group); KBS (low protein diet + KBS-administered group); Arg (low protein diet + Arg-administered group); Glu (low protein diet + Glu-administered group). The mice were fed indicated diet, administered each material three times a week for 12 weeks, housed four to six per cage in a laminar air-flow room, and maintained at a temperature of 22 ± 1 C, a relative humidity of 55 ± 1% throughout the study. The research was conducted in accordance with internationally accepted principles for laboratory animal use and care as found in US guidelines (NIH publication #85-23, revised in 1985).

Table 2. The Ratio of the Components in KBS.

Components	Ratio (%)
1. Hominis Placenta extract	20.70
2. Ceryi Cornu Colla	18.35
3. Acanthopanax Root Bark (Acanthopanax sessiliflorus (Rupr. et Maxim.) Seem.)	9.20
4. Carthami Tinctorii Fructus (Carthamus tinctorius L.)	4.60
5. Atractylodes rhizome white (*Atractylodes ovata* (Thunb.) DC.)	4.60
6. Hoelen cum Pini Radix (*Pachyma hoelen* Rumph)	4.60
7. Rehmanniae Radix et Rhizoma Preparata (*Rehmannia glutinosa* (Gaertn.) Libosch. ex Steud.)	4.60
8. Paeoniae Radix (*Paeonia lactiflora* Pall.)	4.60
9. Angelicae Gigantis Radix (*Angelica gigas* N.)	4.60
10. Astragali Radix (*Astragalus membranaceus* Bunge)	4.60
11. Sojae Semen (*Rhynchosia nulubilis*)	4.60
12. Ostreae Concha (*Ostrea gigas* Thunb.)	4.60
13. Glycyrrhizae Radix (*Glycyrrhiza uralensis* Fisch)	3.45
14. Cnidii Rhizoma (*Cnidium officinale* Makino)	3.45
15. Cinnamomi Ramulus (*Cinnamomum loureirii* Nees.)	3.45
Total	**100.00**

Preparation of KBS

KBS obtained from the Kyungheebaroker Clinic of Korea. Traditional Medicine (Seoul, Republic of Korea) consisted of 15 Korean medicinal drugs (Table 2). Among 15 drugs, Hominis Placenta extract is the most abundant component in KBS. UNICENTA® (UNIMED PHARM, INC., Seoul, Republic of Korea) was substitubed for Hominis Placenta extract, because UNICENTA® is a manufactured medicine using Hominis Placenta collected from hospital. UNICENTA® contains Glu and Arg (manufacturer's specifications). Dilutions were made in distilled water then filtered through a 0.45- m syringe filter.

Enzyme-linked immunosorbent assay (ELISA)

To measure the level of IGF-I in serum, a modified sandwich ELISA method was used (Moon and Kim, 2011; 2012). In brief, 100 l aliquots of anti-mouse IGF-I monoclonal antibody in

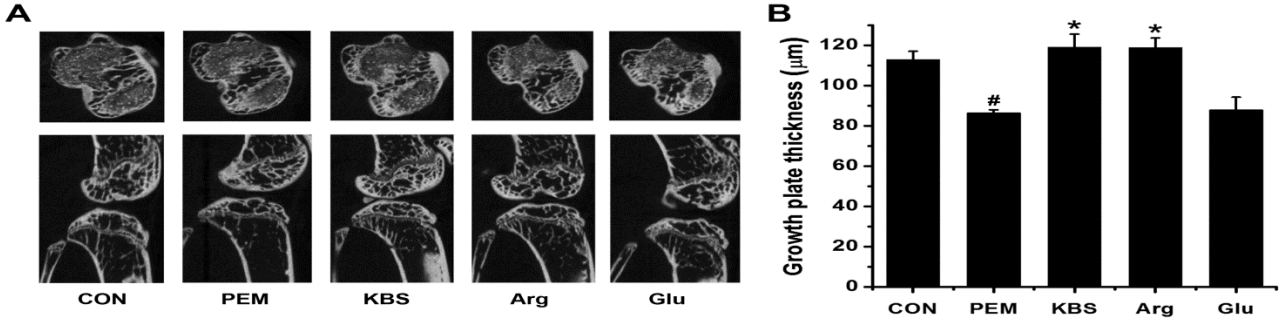

Fig. 1. Effect of KBS on tibial growth plate thickness. (A) Representative 3D μCT images of knee joint showing growth plate. (B) The thickness of excised bone growth plate was determined on five points using the Sky Scan 1076. CON, adequate protein diet + DW-administered group; PEM, low protein diet + DW-administered group; KBS, low protein diet + KBS-administered group; Arg, low protein diet + Arg-administered group; Glu, low protein diet + Glu-administered group. Each datum represents the mean ± SEM of three independent experiments. $^{\#}p < 0.05$; significantly different from the CON value. $^{*}p < 0.05$; significantly different from the PEM value.

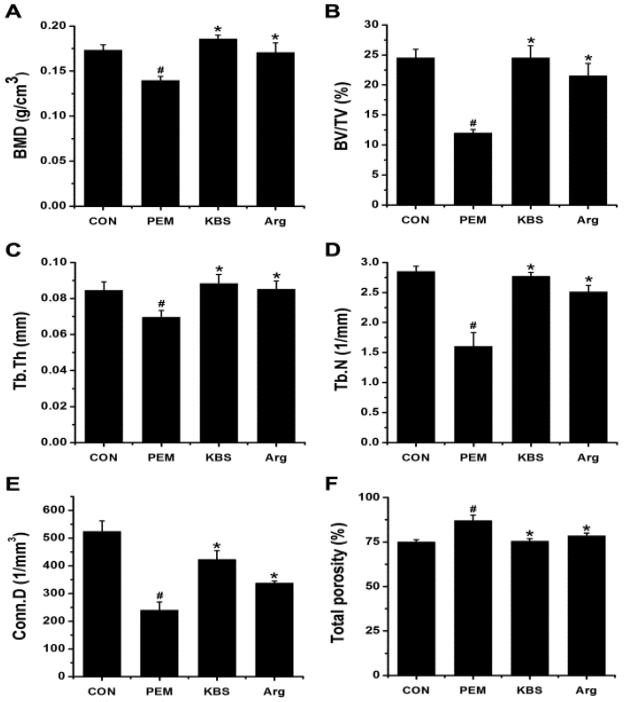

Fig. 2. Effect of KBS on trabecular bone properties. BMD and trabecular parameters of excised bone at the tibia were determined. (A) BMD using 2D μCT. (B-F) Quantified parameters of proximal tibia using 3D μCT. CON, adequate protein diet + DW-administered group; PEM, low protein diet + DW-administered group; KBS, low protein diet + KBS-administered group; Arg, low protein diet + Arg-administered group. Each datum represents the mean ± SEM of three independent experiments. $^{\#}p < 0.05$; significantly different from the CON value. $^{*}p < 0.05$; significantly different from the PEM value.

PBS were coated in 96-well microplate. The plate was incubated overnight at 4 C, washed with PBS containing 0.05% tween-20 (Sigma, St. Louis, MO, USA), and blocked for 1 h with PBS containing 1% BSA, 5% sucrose and 0.05% NaN3. After washing the plates again, avidin-peroxidase was added and the plate was incubated for 30 min at 37 C. The well was again washed and TMB substrate (Pharmingen) was added. Color development was measured at 405 nm using an automated microplate ELISA reader. A standard curve was run on the plate using recombinant mouse IGF-I in serial dilutions.

Polymerase chain reaction (PCR) analysis

Using an easy-BLUETM RNA extraction kit (iNtRON Biotech, Republic of Korea), total RNA was isolated from liver tissues according to the manufacturer's specifications, as previously described (Han et al., 2011; Moon et al., 2012). The concentrations of total RNA in the final elutes were determined by a spectrophotometer. Total RNA (1 g) was heated at 65°C for 10 min and then chilled on ice. Each sample was reverse-transcribed to cDNA for 90 min at 37℃ using a cDNA synthesis kit (Amersham Pharmacia Biotech, Piscataway, NJ, USA). The PCR was performed with the following primer for mouse IGF-I (5' CCG GAC CAG AGA CCC TTT G3'; 5' CCT GTG GGC TTG TTG AAG TAA AA3'); GAPDH (5'GGC AAA TTC AAC GGC ACA3'; 5' GTT AGT GGG GTC TCG CTC CTG3'). Quantitative real-time PCR was performed using a SYBR Green master mix and the detection of mRNA was analyzed using an ABI StepOne real-time PCR System (Applied Biosystems, Foster City, CA, USA). The level of the target mRNA was normalized to the level of the GAPDH and compared with the control. All data were analyzed using the ΔΔCT method.

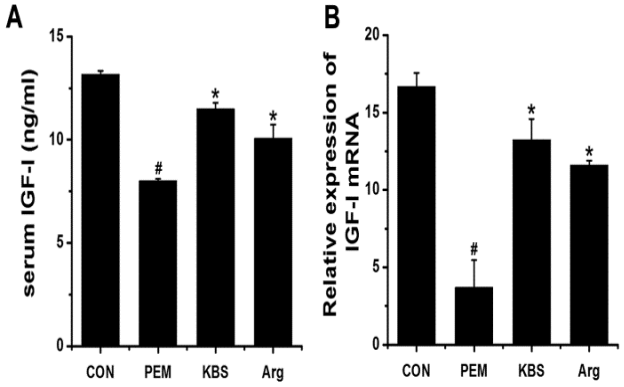

Fig. 3. Effect of KBS on the regulation of IGF-I. (A) IGF-I levels in the serum were measured with the ELISA method. (B) The expression levels of IGF-I mRNA were evaluated by the real-time PCR method. CON, adequate protein diet + DW-administered group; PEM, low protein diet + DW-administered group; KBS, low protein diet + KBS-administered group; Arg, low protein diet + Arg-administered group. Each datum represents the mean ± SEM of three independent experiments. $^{\#}p < 0.05$; significantly different from the CON value. $^{*}p < 0.05$; significantly different from the PEM value.

Western blot analysis

The supernatants of homogenized liver tissues were prepared in a sample buffer containing sodium dodecyl sulfate (SDS). The samples were heated at 95℃ for 5 min and briefly cooled on ice. Following the centrifugation at 15,000 × *g* for 5 min, the proteins in the lysates were separated by 10% SDS-polyacrylamide gel electrophoresis and transferred to nitrocellulose paper. The nitrocellulose paper was blocked with5% skim milk in PBS-tween-20 for 1 h at room temperature and then incubated with primary and secondary antibodies. Finally, the protein bands were visualized by an enhanced chemiluminesence solution purchased from Amersham Co. (Newark, NJ, USA) following the manufacturer's instructions.

Immunohistochemistry

Tissue samples were immediately fixed with 4% formaldehyde and embedded in paraffin. After dewaxing and dehydration, sections were blocked with bovine serum albumin followed by 60 min of incubation with anti–mouse pSTAT5 (Santacruz, CA, USA) at a concentration of 1 μg/ml. The secondary antibody, TRITC-conjugated anti-rabbit IgG (invitrogen), was added to the sections for 30 min. All specimens were examined with a confocal laser-scanning microscope. Sections were coded and randomly analyzed by three blinded observers.

Microcomputed tomography

High-resolution microcomputed tomography (μCT) was used to provide the 2D and 3D information on bone geometry. The mice were sacrificed; femora and tibiae were dissected, cleaned of soft tissue, and fixed in 4% formaldehyde before storage. The source of the open tube type and the minimum focal spot size was 8 μm. Reconstruction was carried out using a modified Feldkamp algorithm using the Sky Scan Nrecon software (Sky Scan, Ltd., Kartuizersweg, Kontich, Belgium). The x-ray source was set at 75 kV and 100 A. Four hundred projections were acquired over an angle of 180°. The image slices were reconstructed using cone-beam reconstruction software based on the Feldkamp algorithm (Dataviewer; Skyscan, Belgium). The trabecular bone was extracted by drawing ellipsoid contours with the CT analyzer software. Trabecular bone volume (BV/TV; percentage) and trabecular number (Tb.N) of femur epiphysis and proximal tibial metaphysis were calculated

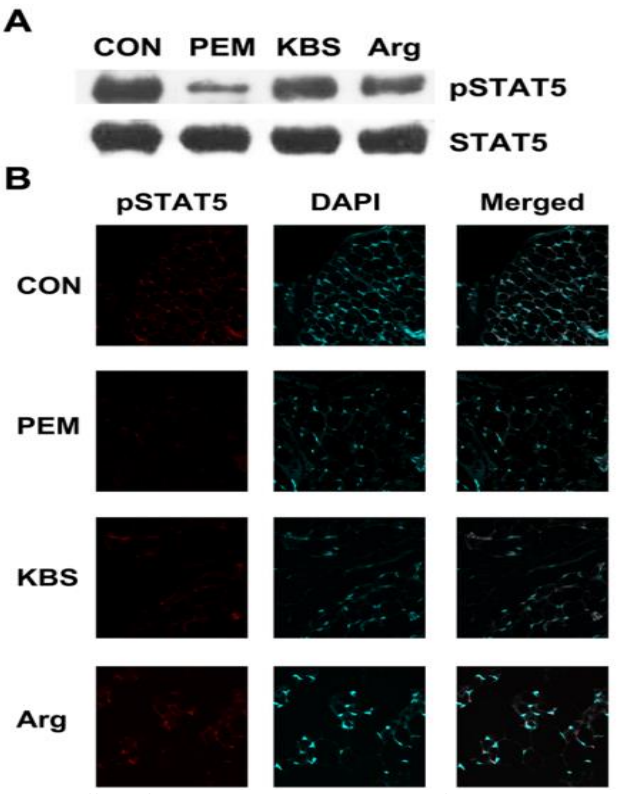

Fig. 4. Effect of KBS on the phosphorylation of STAT5. (A) Liver tissues of each mouse were homogenized and analysed for pSTAT5 and STAT5 by Western blot analysis using specific anti-pSTAT5 and STAT5 antibodies as described in the experimental procedures. (B) pSTAT5 was analyzed by immunohistochemistry in the tibia. CON, adequate protein diet + DW-administered group; PEM, low protein diet + DW-administered group; KBS, low protein diet + KBS-administered group; Arg, low protein diet + Arg-administered group.

by the mean intercept length method. Trabecular thickness (Tb.Th; mm) was calculated according to the method of Hildebrand and Ruegsegger (Ngueguim et al., 2012). 3D parameters were based on analysis of a Marching cubes-type model with a rendered surface. To analyze 3D parameters intibias, whole bone was scanned, and 600 slices of 8 μm in thickness were placed through the former area. Bone volume/ tissue volume (BV/TV), trabecular thickness (Tb.Th), trabecular number (Tb.N), connection density (Conn.D), and total porosity were recorded. The thickness of excised bone growth plate was determined using the Sky Scan 1076 as described in a previously published protocol (Sharan et al., 2011).

Statistical analysis

Statistical analysis was performed using SPSS software (version 14.0, SPSS Inc, Chicago, IL, USA). All results are expressed as the mean ± SEM. The statistical evaluation of the results was performed by an independent t-test. The results were deemed significant at $p < 0.05$.

RESULTS

Effect of KBS or Arg or Glu on growth plate in mice

The proximal tibia growth plate length was measured to examine the longitudinal bone growth using a CT. The lengths of proximal tibia growth plate in the CON and PEM groups were 112.82 4.18 and 86.43 1.47, respectively. The growth plate lengths in the KBS, Arg, and Glu groups were 119.05 6.48, 118.75 4.81, and 87.82 6.38, respectively. KBS and Arg significantly enhanced the longitudinal bone growth, whereas Glu did not (p 0.05, Fig. 1). Thus, we performed subsequent studies with KBS and Arg except for Glu.

Effect of KBS or Arg on trabecular bone parameters

We performed CT measurements to evaluate whether KBS or Arg could affect developmental bone growth. The KBS or Arg-administered mice showed an increase in the bone mineral density (BMD) (Fig. 2A). The 3D μCT reconstruction of trabecular bone images, converted into parameters representing trabecular connectivity, revealed an increase in the BV/TV, Tb.Th, Tb.N, and Conn.D, and a fall in the total porosity at tibia (Fig. 2B-F).

Effect of KBS or Arg on the regulation of IGF-I

To examine whether KBS or Arg can elevate IGF-I level in the serum, we measured the level of IGF-I by means of sandwich ELISA method. The serum IGF-I level was significantly up-regulated by KBS or Arg ($p < 0.05$, Fig. 3A). Then we analyzed the IGF-I mRNA expression in the liver, because majority of plasma IGF-I is biosynthesized in the liver. As expected, hepatic IGF-I mRNA level was found to be significantly elevated in KBS or Arg-administered group ($p < 0.05$, Fig. 3B).

Effect of KBS or Arg on the phosphorylation of STAT5

To determine whether the longitudinal bone growth by KBS or Arg is mediated by the phosphorylation of STAT5, we performed Western blot analysis and immunohistochemistry. As shown in Fig. 4A, the phosphorylation of STAT5 in the liver decreased by malnutrition. However, the decreased STAT5 phosphorylation was up-regulated by KBS or Arg. Furthermore, STAT5 phosphorylation increased by KBS or Arg in the tibia (Fig. 4B).

DISCUSSION

In this study, we have shown that KBS increases the length of growth plate and improves the bone parameters such as BV/TV, Tb.Th, Tb.N, Conn.D, and total porosity. KBS also elevated the level of serum IGF-I through the phosphorylation of STAT5.

Generally, endochondral bone growth initiates at the growth plate cartilage. During normal bone growth, chondrocytes continually mature and produce cartilage at the growth plate to allow bones to lengthen (endochondral bone formation) (Harris et al., 2009). In the present study, KBS increased the thickness of growth plate (Fig. 1). Thus, we can speculate that KBS could be helpful to children who are in retard for their age.

Glucocorticoids are a class of steroid hormones that bind to intracellular glucocorticoid receptors (GRs). In turn, the GR complex migrates to the nucleus where it inhibits nuclear factor (NF)-κB and activator protein (AP)-1 driven gene expression (Barnes, 2006). Moreover, glucocorticoids may suppress granulocyte activation and recruitment, preserve endothelial cell integrity and control vascular permeability (Thompson, 2003). Dexamethasone (Dex) is a synthetic glucocorticoid which shows a 20 to 30 times higher potency to evoke anti-inflammatory effects relative to the endogenously produced cortisol (Blaser et al., 2011). It has been reported that the glucocorticoid Dex has an antiallergic activity and clinical efficacy in allergic diseases (Puigneró et al., 1995; Wershil et al., 1995). Thus, Dex has been proposed as a medication to treat various diseases such as edema, headaches, acute otitis externa, and ocular toxoplasmosis (Brynskov et al., 2013;

Giuliano et al., 2012; Rahman et al., 2007; Soheilian et al., 2011). However, Kugelberg et al. (2005) reported that Dex eye drops inhibit growth in the newborn rabbit. Study by Chrysis et al. (2003) demonstrated that systemic Dex treatment led to a pronounced reduction of the size of the growth plate in tibiae.

Furthremore, Baron et al. (1992) reported that glucocorticoids act locally in the growth plate to inhibit bone growth. It's fortunate that IGF-1 has antiapoptotic actions in lots of tissues and may therefore have a potential to prevent glucocorticoid-induced chondrocyte apoptosis. It was reported that IGF-I prevents dexamethasone-induced apoptosis and suppression of chondrocyte proliferation (Chrysis et al., 2005). Our results showed that KBS increases the serum IGF-I level (Fig. 3). Thus, we can presume that KBS could partially recover the growth retardation by Dex through the elevation of IGF-I level.

KBS is consisted of 15 Korean medicinal drugs. Among 15 drugs, Hominis Placenta protected osteoporosis in ovariectomized rats (Chae et al., 2006). Carthami Tinctorii Fructus increased the level of serum IGF-I and lengths of femur and tibia, however, its effect was very small and transient (Lee et al., 2009). Kim et al. (2002) reported that Carthami Tinctorii Fructus partially prevents ovariectomy-induced bone loss. However, the effect of individual drug was less than those of all drugs, prescription KBS.

In conclusion, the present study demonstrated that KBS increases the length of growth plate and improves the bone parameters. KBS also elevated the level of serum IGF-I through the phosphorylation of STAT5. Overall, this study suggests that KBS would be helpful to children who are in retard for their age through the elevation of IGF-I.

ACKNOWLEDGEMENTS

This research was supported by Kyung Hee University in 2013.

CONFLICT OF INTEREST

The authors report no declarations of interest.

REFERENCES

Abad V, Meyers JL, Weise M, Gafni RI, Barnes KM, Nilsson O, Bacher JD, Baron J. The role of the resting zone in growth plate chondrogenesis. Endocrinology. 2002;143:1851-1857.

Barnes PJ. How corticosteroids control inflammation: Quintiles Prize Lecture 2005. Br J Pharmacol. 2006;148:245-254.

Baron J, Huang Z, Oerter KE, Bacher JD, Cutler GB Jr. Dexamethasone acts locally to inhibit longitudinal bone growth in rabbits. Am J Physiol. 1992;263:E489-E492.

Blaser C, Wittwer M, Grandgirard D, Leib SL. Adjunctive dexamethasone affects the expression of genes related to inflammation, neurogenesis and apoptosis in infant rat pneumococcal meningitis. PLoS One. 2011;6:e17840.

Brooks AJ, Waters MJ. The growth hormone receptor: mechanism of activation and clinical implications. Nat Rev Endocrinol. 2010;6:515-525.

Brynskov T, Laugesen CS, Halborg J, Kemp H, Sørensen TL. Longstanding refractory pseudophakic cystoid macular edema resolved using intravitreal 0.7 mg dexamethasone implants. Clin Ophthalmol. 2013;7:1171-1174.

Chae HJ, Choi KH, Chae SW, Kim HM, Shin TK, Lee GY, Jeong GS, Park HR, Choi HI, Kim SB, Yoo SK, Kim HR. Placenta hominis protects osteoporosis in ovariectomized rats. Immunopharmacol Immunotoxicol. 2006;28:165-173.

Choi MJ, Chang KJ. Effect of dietary taurine and arginine supplementation on bone mineral density in growing female rats. Adv Exp Med Biol. 2013;776:335-345.

Chrysis D, Ritzen EM, Sävendahl L. Growth retardation induced by dexamethasone is associated with increased apoptosis of the growth plate chondrocytes. J Endocrinol. 2003;176:331-337.

Chrysis D, Zaman F, Chagin AS, Takigawa M, Sävendahl L. Dexamethasone induces apoptosis in proliferative chondrocytes through activation of caspases and suppression of the Akt-phosphatidylinositol 3'-kinase signaling pathway. Endocrinology. 2005;146:1391-1397.

Davey HW, Park SH, Grattan DR, McLachlan MJ, Waxman DJ. STAT5b-deficient mice are growth hormone pulse-resistant. Role of STAT5b in sex-specific liver p450 expression. J Biol Chem. 1999;274:35331-35336.

de Vos AM, Ultsch M, Kossiakoff AA. Human growth hormone and extracellular domain of its receptor: crystal structure of the complex. Science. 1992:255:306-312.

Fock RA, Rogero MM, Vinolo MA, Curi R, Borges MC, Borelli P. Effects of protein-energy malnutrition on NF-kappaB signalling in murine peritoneal macrophages. Inflammation. 2010;33:101-109.

Giuliano C, Smalligan RD, Mitchon G, Chua M. Role of dexamethasone in the prevention of migraine recurrence in the acute care setting: a review. Postgrad Med. 2012;124:110-115.

Han NR, Kim HM, Jeong HJ. Kanamycin activates caspase-1 in NC/Nga mice. Exp Dermatol. 2011;20:659-663.

Harris L, Senagore P, Young VB, McCabe LR. Inflammatory bowel disease causes reversible suppression of osteoblast and chondrocyte function in mice. Am J Physiol Gastrointest Liver Physiol. 2009;296:G1020-G1029.

Kim HJ, Bae YC, Park RW, Choi SW, Cho SH, Choi YS, Lee WJ. Bone-protecting effect of safflower seeds in ovariectomized rats. Calcif Tissue Int. 2002;71:88-94.

King B, Jiang Y, Su X, Xu J, Xie L, Standard J, Wang W. Weight control, endocrine hormones and cancer prevention. Exp Biol Med. 2013;238:502-508.

Kugelberg M, Shafiei K, Ohlsson C, Sävendahl L, Zetterström C. Glucocorticoid eye drops inhibit growth in the newborn rabbit. Acta Paediatr. 2005;94:1096-1101.

Le Roith D, Bondy C, Yakar S, Liu JL, Butler A. The somatomedin hypothesis: 2001. Endocr Rev. 2001;22:53-74.

Lee YS, Choi CW, Kim JJ, Ganapathi A, Udayakumar R, Kim

SC. Determination of mineral content in methanolic safflower (Carthamus tinctorius L.) seed extract and its effect on osteoblast markers. Int J Mol Sci. 2009;10:292-305.

Lui JC, Baron J. Effects of glucocorticoids on the growth plate. Endocr Dev. 2011;20:187-193.
Moon PD, Choi IH, Kim HM. Epigallocatechin-3-O-gallate inhibits the production of thymic stromal lymphopoietin by the blockade of caspase-1/NF-κB pathway in mast cells. Amino Acids. 2012;42:2513-2519.

Moon PD, Kim HM. Thymic stromal lymphopoietin is expressed and produced by caspase-1/NF-κB pathway in mast cells. Cytokine. 2011;54:239-243.

Moon PD, Kim HM. Suppression of thymic stromal lymphopoietin production by rutin in mast cells. Food Chem. 2012;133:76-81.

Ngueguim FT, Khan MP, Donfack JH, Siddiqui JA, Tewari D, Nagar GK, Tiwari SC, Theophile D, Maurya R, Chattopadhyay N. Evaluation of Cameroonian plants towards experimental bone regeneration. J Ethnopharmacol. 2012;141:331-337.

Pennisi P, Clementi G, Prato A, Luca T, Martinez G, Mangiafico RA, Pulvirenti I, Muratore F, Fiore CE. L-arginine supplementation normalizes bone turnover and preserves bone mass in streptozotocin-induced diabetic rats. J Endocrinol Invest. 2009;32:546-551.

Puigneró V, Salgado J, Queralt J. Effects of cyclosporine and dexamethasone on IgE antibody response in mice, and on passive cutaneous anaphylaxis in the rat. Int Arch Allergy Immunol. 1995;108:142-147.

Rabkin R, Sun DF, Chen Y, Tan J, Schaefer F. Growth hormone resistance in uremia, a role for impaired JAK/STAT signaling. Pediatr Nephrol. 2005;20:313-318.

Rahman A, Rizwan S, Waycaster C, Wall GM. Pooled analysis of two clinical trials comparing the clinical outcomes of topical ciprofloxacin/dexamethasone otic suspension and polymyxin B/neomycin/hydrocortisone otic suspension for the treatment of acute otitis externa in adults and children. Clin Ther. 2007;29:1950-1956.

Reeves PG, Nielsen FH, Fahey GC Jr. AIN-93 purified diets for laboratory rodents: final report of the American Institute of Nutrition ad hoc writing committee on the reformulation of the AIN-76A rodent diet. J Nutr. 1993;123:1939-1951.

Sharan K, Mishra JS, Swarnkar G, Siddiqui JA, Khan K, Kumari R, Rawat P, Maurya R, Sanyal S, Chattopadhyay N. A novel quercetin analogue from a medicinal plant promotes peak bone mass achievement and bone healing after injury and exerts an anabolic effect on osteoporotic bone: the role of aryl hydrocarbon receptor as a mediator of osteogenic action. J Bone Miner Res. 2011;26:2096-2111.

Soheilian M, Ramezani A, Azimzadeh A, Sadoughi MM, Dehghan MH, Shahghadami R, Yaseri M, Peyman GA. Randomized trial of intravitreal clindamycin and dexamethasone versus pyrimethamine, sulfadiazine, and prednisolone in treatment of ocular toxoplasmosis. Ophthalmology. 2011;118:134-141.

Thompson BT. Glucocorticoids and acute lung injury. Critl Care Med. 2003;31:S253-S257.

Weng CY, Kothary PC, Verkade AJ, Reed DM, Del Monte MA. MAP kinase pathway is involved in IGF-1-stimulated proliferation of human retinal pigment epithelial cells (hRPE). Curr Eye Res. 2009;34:867-876.

Wershil BK, Furuta GT, Lavigne JA, Choudhury AR, Wang ZS, Galli SJ. Dexamethasone or cyclosporin A suppress mast cell-leukocyte cytokine cascades. Multiple mechanisms of inhibition of IgE- and mast cell-dependent cutaneous inflammation in the mouse. J Immunol. 1995;154:1391-1398.

Woelfle J, Chia DJ, Rotwein P. Mechanisms of growth hormone (GH) action. Identification of conserved Stat5 binding sites that mediate GH-induced insulin-like growth factor-I gene activation. J Biol Chem. 2003;278:51261-51266.

Youreva V, Kapakos G, Srivastava AK. Insulin-like growth-factor-1-induced PKB signaling and Egr-1 expression is inhibited by curcumin in A-10 vascular smooth muscle cells. Can J Physiol Pharmacol. 2013;91:241-247.

Zhang R, Ruan D, Zhang C. Effects of TGF-beta1 and IGF-1 on proliferation of human nucleus pulposus cells in medium with different serum concentrations. J Orthop Surg Res. 2006;1:9.